

Short-term Prediction and Detection of Dynamic Atmospheric Phenomena by Microwave Radiometer

Petr DVORAK, Milos MAZANEK, Stanislav ZVANOVEC

Dept. of Electromagnetic Field, Czech Technical University in Prague, Technicka 2, 166 27 Prague 6, Czech Republic

petr.dvorak@fel.cvut.cz, mazanekm@fel.cvut.cz, xzvanove@fel.cvut.cz

Abstract. *Specific utilization of a microwave radiometer for online monitoring, detection and, especially, prediction of particular dynamic atmospheric phenomena such as precipitation and cloudiness is proposed in the paper. The ground-based microwave radiometer and meteorological stations were incorporated into the measurement campaign in order to observe and analyze actual brightness temperature changes. The characteristics of atmospheric parameters recorded over a period of 14 months were evaluated and new applications for rain forecasting and cloud detection, using specific features of signal variance, were proposed and validated.*

Keywords

Microwave radiometer, rain detection, cloud detection, wave propagation.

1. Introduction

Microwave radiometers have been used as ground or satellite-based instruments for the measurement of temperature radiation emitted by objects, the Earth's surface, and for the monitoring of background space or atmospheric noise for tens of years [1]. Several different types of radiometers can be distinguished based on their operating frequency, type of measured medium, application, etc. [2], [3], [4], [5].

Even though radiometric measurements have been performed for decades and many phenomena were thoroughly described, today's technological enhancements still open up new research challenges. This is especially true with the movement to higher frequency bands (millimeter, THz [6], optical or hybrid RF/optical [7]) allowing the utilization of higher data rates. Nonetheless, the availability of these emerging millimeter communication systems is essentially influenced by dynamic atmospheric phenomena such as rain [7], [8]. Due to the higher costs of the technology for these communication systems, there is a strong requirement for the prediction of undesirable atmospheric events in order to accommodate appropriate fade mitigation techniques. Since radiometric systems can even be built as a monolithic microwave integrated circuits

(MMIC) the future high-end wireless communication links could be equipped with a low-cost radiometer [9] to measure and predict in advance any atmospheric phenomena that might affect the reliability of the link.

Atmospheric changes are typically observed by radiometers, mainly in the 22 – 30 GHz band around the water vapor resonance and then in the 51 – 59 GHz resonant oxygen band. A general description of brightness temperature and rain statistics was presented by Hogg in [10]. The dependence of the brightness temperature and rain intensity database (simulated) was analyzed from the air by Meneghini in [11] using the maximum a posterior probability criterion. The retrieval of rain and cloud parameters from space-borne radiometer measurements was well described by Pierdicca [12], Burns [13] and Westwater [14]. An estimation of rainfall rates and columnar hydrometeor contents from joint measurement data from a spaceborne radiometer and radar was proposed by Marzano et al in [15], [16]. Nowcasting of rain events from satellite microwave and infrared sensor imagery (e.g. for emergency issues) was investigated by Marzano et al. in [17]. Rainfall prediction based on ground-based microwave radiometer measurements was proposed by Liu [18]. Won [19] used a method where rainfall data were moving – accumulated – in 15 minute periods and the algorithm considered a possible rain event within the following 2 hours. However, as it was well highlighted by authors, only very few rain events were analyzed and therefore the results were not so straightforward. Other methods utilize a steady threshold to predict rain events [20], however their proper validation has not yet been clearly investigated and confirmed.

In order to determine general atmospheric conditions in a particular area, analyses of atmospheric brightness temperatures measured by a ground-based radiometer over a period of 14 months are presented in the paper. Thanks to the long-term monitoring, whole season statistics over a wide temperature range were evaluated. Based on specific brightness temperature measurements of selected atmospheric phenomena (in particular those associated with rainfalls or water content), meteorological characteristics were classified and new measuring methods were proposed.

The paper is structured according to the following scheme. Measuring systems are briefly described in Sec-

tion 2. Dependencies of measured brightness temperatures on precipitation, temperature data and clouds' presence are then analyzed in Section 3. Detection and prediction methods for precipitation are afterwards tested and an improved approach is proposed. The following subsection elaborates cloudiness detection. Finally, a brief conclusion summarizes the results obtained and methodology used.

2. Measuring Systems

In order to validate brightness temperature changes and to obtain better statistical insight, an experimental study was set up in the university campus of the Faculty of Electrical Engineering, Czech Technical University in Prague (CTU), Czech Republic. The experimental measuring system consists of a ground based radiometric station and a set of weather sensors located at two meteorological stations.

2.1 Microwave Radiometer

The microwave radiometer based on the Dicke switch design [21] was utilized for long-term monitoring of brightness temperature. Using the band at frequencies lower than 37 GHz leads to measurements of the brightness temperature that respond more to rain or cloud liquid emissions. The lower working frequency range of 10.95 - 12.75 GHz (satellite band) was chosen to measure the thermal deviation for two main reasons – we wanted to avoid the strong absorption line of water vapor in the atmosphere at 22 GHz, which would cause partial biasing of measurement results, and secondly because of the availability of technology for satellite receivers. When using band with frequencies higher than 37 GHz, brightness temperature mainly responds to cloud ice scattering [22].

The vertically pointed radiometer was deployed on the roof of the CTU building, 36 m above the ground level, therefore it was well isolated with respect to the brightness temperature contribution in a given antenna (receiving) radiation pattern of received noise signal from adjacent buildings. The radiometer exterior and internal deployments are shown in Fig. 1 - the parabolic antenna of the radiometer points towards a tilted planar mirror. This arrangement was chosen in order to avoid antenna aperture aggradations by any impurities that could affect signal measuring. The metal mirror was also smeared with a hydrophobic film of silicon oil in order to trickle water drops away. The chosen arrangement allows a pure vertical distribution of the ice and liquid content of clouds to be obtained and analyzed.

In the Dicke design, the radiometer switches in turn between the antenna output and the reference (temperature stabilized) load. After the signal has passed through internal amplifiers and a detector, part of the signal is detected at the switching frequency by a synchronous detector. The output signal of the synchronous detector is proportional to

the difference of the brightness temperature of an observed object and the reference load. The radiometer principle used introduces a higher level of stability and sensitivity at the expense of reduced thermal sensitivity. The switching of the gain with calibration was also used in order to avoid saturation. Temperatures of particular subsystems in the radiometer are measured and used for the continuous correction of measured data. The radiometer has a floating reference whose temperature changes are substantially slower than the changes in measured brightness temperature. The temperature stability of the reference load is given by a robust and thermally insulated construction where the temperature is also measured. The time constant of the reference load is more than ten times higher than the time constant of the measured object. Therefore, there is no need ever to calibrate the equipment after the first laboratory calibration. The use of another type of radiometer such as a total power radiometer or a noise injection radiometer was also considered at the very beginning of the measurement campaign; however the Dicke design was selected as the best compromise, providing good sensitivity and acceptable stability without any follow-up calibration [3]. Some undesirable signals can affect the measurement, such as heating of the radiometer housing or mirror heating, but these effects were suppressed by temperature corrections of the radiometer and by a proper detection method (as described in more depth in Section 3.2).



Fig. 1. 1a) Photographs of the tilted planar mirror and the case with the radiometer placed on the roof; b) the inner deployment of the microwave radiometer.

Radiometer bandwidth	1.7 GHz
Integration time	0.5 ms
Radiometer sensitivity	1.4 K
Antenna beamwidth (-3 dB)	4 deg
Sidelobe level	>20 dB
Switching frequency	1 kHz
Measuring data averaging interval *	3 s
GPS Location:	50.10339, 14.392749

Tab. 1. Main properties of the radiometer (*all cycles in this period are averaged).

2.2 Meteorological Station

Data from two (primary and backup) meteorological stations WS981, made by the Anemo Corporation, Czech Republic [23], have been used for further analysis. Each station collects the temperature and humidity, as well as atmospheric pressure (barometer TMAG 518N4F with

range 800 – 1200 hPa), precipitations (heated tipping-bucket rain gauge with a collecting area of 500 cm², and the rain amount per one tip of 0.1 mm), and the speed and direction of the wind (anemometer AN 955C). The primary meteorological station is located at same place as the radiometer, i.e. 36 m above ground level. Measurement data are collected in 1 minute intervals, therefore to harmonize the sampling of meteorological and radiometer data, the 3 second intervals of radiometer data were averaged over 1 minute. Only measurements of temperature and precipitation were used for direct processing.

3. Results and Discussion of Measured Statistics

In this section, the relation between measured brightness temperature and weather conditions will be discussed. Nevertheless, the terminology of the detection methods first has to be defined.

Hereafter, "Hit" indicates that the precipitation was observed after it had been predicted; "Miss" then means that the precipitation was observed even though it had not been predicted. "False alarm" stands for a situation when precipitation had been predicted but did not occur (see Tab. 2).

Event forecast		
Yes		No
Event observation		Event observation
Yes	No	Yes
Hit	False Alarm	Miss

Tab. 2. Terminology contingency table.

Measured data were analyzed over the period of 14 months, from March 2010 to April 2011. During this period 314 clearly defined atmospheric states were observed. These states can be detected or predicted by a microwave radiometer with the use of the proper statistical tools. To achieve the best results the method with variance enumeration was proposed.

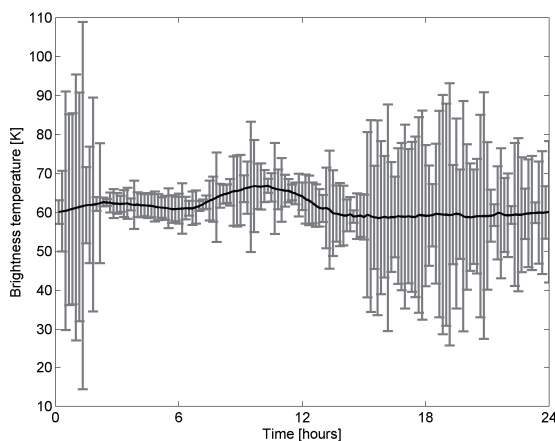


Fig. 2. Diurnal brightness temperature changes with marked standard deviation.

The basic statistics of measured brightness temperature - medium curve of average diurnal brightness temperature calculated over 499 days depicted with a standard deviation range - is shown in Fig. 2.

3.1 Precipitation Detection and Prediction

The main aim of the paper is to introduce the detection of dynamic atmospheric events that are connected with certain atmospheric states. Initially, the utilization of a microwave radiometer as a precipitation detector and especially for precipitation prediction was investigated. Different types of clouds as well as various precipitation events were observed and recorded during the measuring period. It was derived – similarly as it was described by Won in [19] – that during a particular time interval before the start of a rain event a rapid increase of the brightness temperature can be observed. Contrary to [19], where only small number of events was analyzed, 69 rain events were recorded over the entire period during the 10 GHz radiometer measuring campaign at the CTU.

A simple approach using a steady threshold to predict rain events [20] was dismissed at the beginning of analysis because it had led to a higher number of "False alarms". In Fig. 3 a typical situation is depicted on the set of precipitation and brightness temperature data. In this simple (generally used) steady threshold method of cloud or rain event detection, a particular threshold is first carefully determined. When the brightness temperature exceeds the threshold limit, an event is predicted (Hit indication).

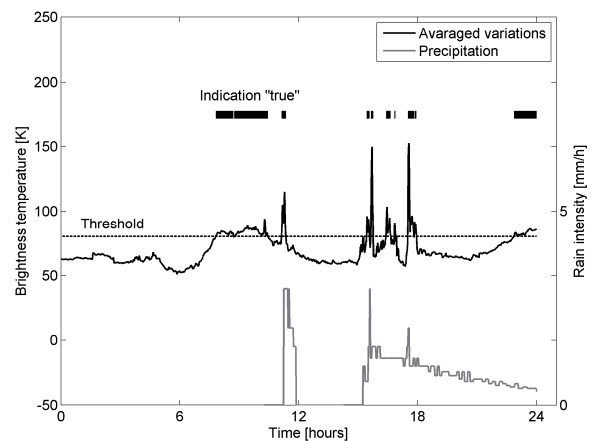


Fig. 3. Example of simple threshold method utilization for the prediction of rain events; data from 24th of May 2010.

The main problem arises with the threshold determination. When a low threshold is chosen to achieve extremely sensitive forecasting (i.e. for radiometer measurements in time intervals shorter than 1 minute), a number of "False alarm" signals are usually generated. By establishing a higher threshold we can on the one hand rapidly reduce the number of false alarms, but on the other hand, as it was confirmed by our analyses, this causes more "Misses" and, what is more, it inconveniently shortens the forecasting period before events. In other words, in many cases it

results in the degradation of forecasting information. An example of false alarm signals observed on 24th May, 2010 before 12.00 (note: all measurement records are related to UTC) can be distinguished in Fig. 3. In this case, the threshold was set to a value of 80 K of brightness temperature.

Since the success rate of the method analyzed above had not proved satisfactory, a more reliable detecting method based on observations that the rapid increase of brightness temperature precedes rain events was proposed. The new method inheres in brightness temperature variances calculated over a particular time window within the measuring period. By parametric study, a 5 minute window of variance calculation was found to be the most effective. A shorter window results in higher variances even for non-significant events e.g. an artificial ripple in the brightness temperature, while with a longer window the forecasting information degrades or is lost. To smooth the variance curve, an additional moving average over the 15 minute time window can be applied (note this is not as significant as the first moving average to obtain variances, the 15 minute interval was optimized based on measured data). After these operations the detection threshold can be determined. The advantage of using the variances in this method is in the obvious suppression of slow brightness temperature changes. In this way, variance is also free from the absolute value of measured brightness temperature. The same situation as in Fig. 3 is newly demonstrated in Fig. 4, where the threshold was applied to the curve obtained by moving-averaged variances. It can clearly be seen that false alarm signals were suppressed, and only real rain events could be detected in advance without a significant number of false signals.

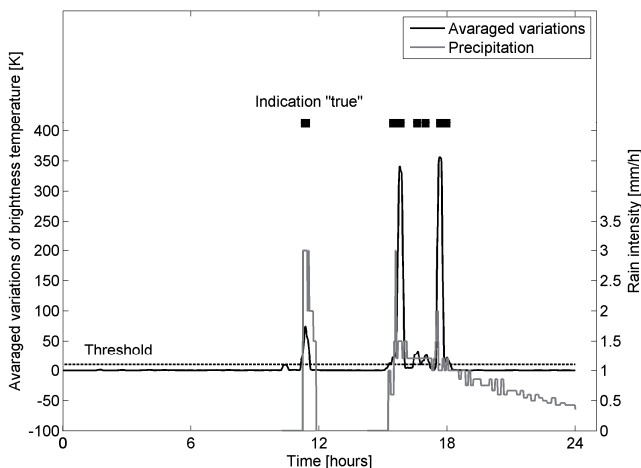


Fig. 4. Example of undesirable signals suppression and rain prediction by using the method proposed in this contribution; data from 24th May, 2010.

The probability of the successful utilization (hit rate) of the proposed method applied to the whole data set (314 events were considered) is summarized in Tab. 3. The whole range of temperature variations thresholds was scanned and the optimum of 10 K was determined as the value corresponding to the highest and the most stable hit rate over the evaluated period.

Threshold	Event forecast		
	Yes		No
	Event observation		Event observation
	Yes (Hit)	No (False alarm)	No (Miss)
8 K	75.4 %	11.7 %	12.9 %
9 K	75.1 %	11.35 %	13.6 %
10 K	74.4 %	7.7 %	17.9 %
11 K	70.1 %	7.5 %	22.4 %
12 K	59.5 %	7.3 %	33.2 %

Tab. 3. Hit rate of precipitation forecasting by the proposed method.

To determine the average forecasting time before rain detection at ground level (note this can be for short intervals more precisely expressed as a detection time), a cross-correlation function was used. Every pattern of events was correlated to the function processed for forecasting (variation, averaging) and the correlation was calculated for different time shifts. The maximum of the cross-correlation product and corresponding forecasting time was derived (see Fig. 5). The average time of the event forecast before the start of precipitation is 1.8 minutes. Since the variance is calculated over a moving time window of measured data, the result of averaging is delayed to brightness temperature changes. Note that the real peaks of brightness temperature can be observed quite some time before the start of rain (approximately 10 minutes). The forecasting time of 1.8 minutes represents a compromise value and corresponds to an acceptable number of Hits and False alarms. There is also a certain degree of freedom, and therefore it is possible to choose between a relatively improved forecasting time, but at the cost of a higher number of False alarms or Missed events. The forecasting time is shortened because of the averaging.

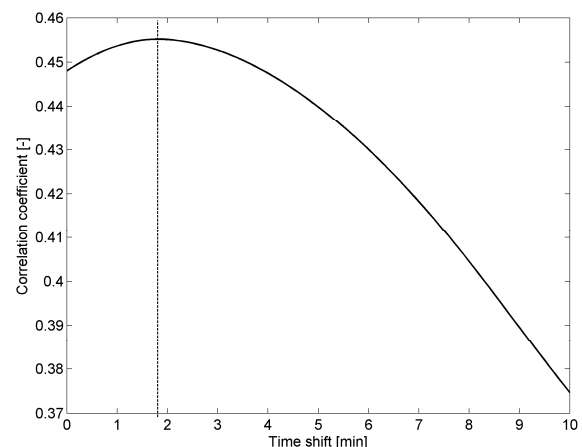


Fig. 5. Averaged cross-correlation products of all rain events.

3.2 Cloudiness Detection

After eliminating the influence of rain, brightness temperature measured by the microwave radiometer and meteorological data was further analyzed. Despite a high randomness rate in the meteorological data, some particularly interesting relationships were observed. At first, the

brightness temperature varied from 47 K up to 65 K, even during periods of clear skies. The amplitude of the measured brightness temperature was dependent on sunshine, i.e. in the daytime. Almost all the higher brightness temperatures with more rapid brightness temperature changes were related to specific types of cloudiness [24] (for cloudiness types see [25]). These issues were also partially described by Long in [26].

Before any discussion of measured data, it was necessary to clarify how the range of measured brightness temperature conforms to certain types of cloudiness. During the measuring campaign several types of clouds (described below) were observed. The types of clouds were determined periodically by the meteorological station service and their base was measured by a ceilometer. Corresponding brightness temperatures were assigned to cloud types. Cumulus clouds are specific with their clearly defined base formed in low altitudes – up to 2.5 km. These clouds have a particularly vertical extent. Cumulus is created by small water drops and can be a source of short-term rainfall. The specific brightness temperature measured in the case of Cumulus clouds varied from 48 K to 55 K. Cumulus clouds can grow into Cumulonimbus – a dense storm cloud with a wide base. This type of cloud is formed at low altitudes from hundreds of meters up to 20 km and can be a significant source of rainfall. The measured brightness temperature of Cumulonimbus clouds was slightly higher than the previous clouds, from 50 K up to 70 K. It was hard to distinguish which brightness temperature is related to Cumulus and Cumulonimbus, but for possible joint microwave links, it is essential that both types of clouds can be a source of rainfall. There is another cloud type with a very low altitude, wide base and small vertical extent – the Stratus cloud. The measured brightness temperature of this cloud varied from 50 K up to 80 K. Other types of clouds formed in high altitudes – Altostratus, Altocumulus and Cirrus – were omitted from the analyses as they do not cause significant changes in measured temperature because the water content of these clouds is much lower than that of the clouds mentioned above.

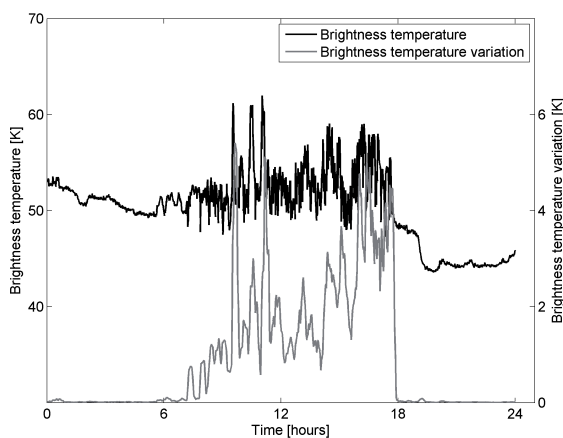


Fig. 6. Typical variations of the brightness temperature during clouds' presence in the monitored volume of atmosphere on 5th April, 2010.

For cloudiness detection, a similar technique was used as for precipitation prediction. This method exploits the instability of brightness temperature when a cloud moves through the observed volume. Again, the variance of the brightness temperature was calculated within a 5 minute time window over the entire period.

A typical behavior pattern for brightness temperature is depicted in Fig. 6, where the clouds' presence in the monitored volume of atmosphere from 7.00 to 18.00 caused higher variations of the brightness temperature.

Variations of brightness temperature are depicted as a function of ambient temperature in Fig. 7 (156 events were captured). The incidence of low temperature can be observed. From the measurements it was found that when the ambient temperature is above 0 °C, the variation of brightness temperature due to the cloud presence is higher – in the range from 0.2 to 4 K. It should be emphasized that when the ambient temperature is below 0 °C, the variation ranges from 0 to 0.5 K. The temperature at ground level (measured by the weather station) is highly correlated to the temperature in the monitored volume of atmosphere above (obtained from the radiometer). Since the radiometer is thermally stabilized, possible slow and minor temperature deviations cannot significantly affect the measurements. To ensure correct interpretation of the results, the influence of temperature (below/above 0°) is considered and the results are described for both temperature ranges.

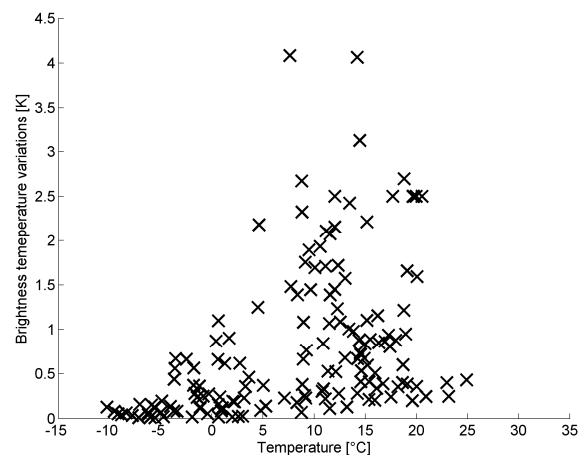


Fig. 7. Brightness temperature variations when clouds passed through the vertical volume monitored by the radiometer.

In Fig. 8, variation of brightness temperature is shown in a situation without clouds in the monitored volume of atmosphere – 158 events were captured during the cloudless period. The contrast with the cloudy case (Fig. 7) is obvious. The variation does not exceed the value of 0.25 K during the cloudless period. Variations, based on measurements when clouds were in the observed volume, can be clearly separated from the state when no clouds were present in the observed volume, and hence a method to detect cloudiness based on the calculation of variations can be proposed.

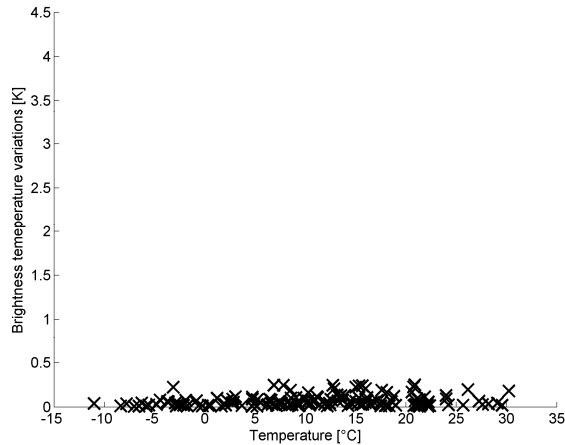


Fig. 8. Brightness temperature variations when no clouds were present in the monitored volume of atmosphere.

The threshold of brightness temperature variations for the determination of cloud presence was parametrically determined as 0.23 K. Using this value as a decision-making parameter, the following results listed in Tab. 4 for temperatures higher than 0 °C were obtained from an analysis of 14 months of measurement data (314 captured events). The hit rate of estimates is substantially higher than the hit rate of estimates calculated for ambient temperature below 0 °C, when the method cannot be properly applied. In such cases the hit rate was only 31.43%.

		Event forecast	
		Yes	No
Event observation	Yes	80.5 %	4.8 %
	No	14.7 %	-

Tab. 4. Hit rate of cloudiness forecasting when the temperature was higher than 0 °C.

4. Conclusion

Based on data measured by the microwave radiometer and adjacent weather station, methods for precipitation detecting and prediction and cloudiness detection were proposed. By utilizing the proposed thresholds of brightness temperature variation, up to 49% increase in precision of precipitating clouds and precipitation detection via 10 GHz radiometer observation can be obtained.

The derived results could enable the development of more reliable wireless communication systems equipped with low-cost radiometers or the use of low-cost radiometers as an additional measuring instrument for meteorological stations.

Based on the water emissivity analysis from the complex permittivity, one can derive the temperature dependence dominating in the 30 GHz band. A frequency band of 2 GHz allows for identification of additives (e.g. salinity) and the 10 GHz band covers both parameters. Subsequent research will be focused on the use of advanced techniques of data mining in order to obtain more accurate and precise measurements. Currently, a 37 GHz radiometer is under

development. This higher band is more suitable for pure temperature deviations corresponding to the emissivity of water [22]. The next steps to achieve more accurate results will involve the use of adaptive data filtering and dynamic on-line threshold determining. The long-term measuring campaign continues and future results will be presented.

Acknowledgements

This research project forms part of the activities of the Department of Electromagnetic Field of the Czech Technical University in Prague within the frames of ICT COST Action IC1101 (supported by the Ministry of Education, Youth and Sports of the Czech Republic grant LD12058). The measurement campaign is supported by the Grant Agency of the Czech Technical University in Prague, grant No. SGS12/142/OHK3/2T/13.

References

- [1] DICKE, R. H. A Radiometer for measuring thermal radiation at microwave frequencies, *Physical Review*, 1946, vol. 69, p. 694 to 694.
- [2] ULABY, F. T., et al. Microwave remote sensing: active and passive. Reading, Mass.: Addison-Wesley Pub. Co., Advanced Book Program/World Science Division, 1981.
- [3] EWANS, G., MCLEISH C. W., *RF Radiometer Handbook*. Dedham: Artech House Inc., 1976.
- [4] BRUSSAARD, G. *Radiometry, A Useful Prediction Tool*. Noordwijk: ESA Scientific and Technical Publ. Branch, ESTEC, NL, 1985.
- [5] ESEPKINA, N. A., KOROLKOV, D. V., PARIJSKIJ, Y. N. *Radiotelesopes and radiometers*. M. Nauka, 1973.
- [6] KAO-CHENG, H., ZHAOCHENG, W. Terahertz terabit wireless communication. *Microwave Magazine*, IEEE, 2011, vol. 12, p. 108-116.
- [7] NADEEM, F., et al. Weather effects on hybrid FSO/RF communication link. *IEEE Journal on Selected Areas in Communications*, 2009, vol. 27, p. 1687-1697.
- [8] ZVANOVEC, S., PIKSA, P., MAZANEK, M., PECHAC, P. A study of gas and rain propagation effects at 48 GHz for HAP scenarios. *EURASIP Journal on Wireless Communications and Networking*, vol. 2008, Article ID: 734216.
- [9] BORGARINO, M., POLEMI, A., MAZZANTI, A. Low-cost integrated microwave radiometer front-end for industrial applications. *IEEE Transactions on Microwave Theory and Techniques*, Dec. 2009, vol. 57, no. 12, p.3011-3018.
- [10] HOGG, D. C. Rain, radiometry, and radar. *IEEE Transactions on Geoscience and Remote Sensing*, Sep 1989, vol. 27, no. 5, p. 576 to 585.
- [11] MENEGHINI, R., KUMAGAI, H., WANG, J. R., IGUCHI, T., KOZU, T. Microphysical retrievals over stratiform rain using measurements from an airborne dual-wavelength radar-radiometer. *IEEE Transactions on Geoscience and Remote Sensing*, May 1997, vol. 35, no. 3, p.487-506.

- [12] PIERDICCA, N., MARZANO, F. S., D'AURIA, G., BASILI, P., CIOTTI, P., MUGNAI, A. Precipitation retrieval from spaceborne microwave radiometers based on maximum a posteriori probability estimation. *IEEE Transactions on Geoscience and Remote Sensing*, Jul 1996, vol. 34, no. 4, p. 831-846.
- [13] BURNS, B. A., WU, X., DIAK, G. R. Effects of precipitation and cloud ice on brightness temperatures in AMSU moisture channels. *IEEE Transactions on Geoscience and Remote Sensing*, Nov 1997, vol. 35, no. 6, p. 1429-1437.
- [14] WESTWATER, E. R. The accuracy of water vapor and cloud liquid determinations by dual-frequency ground-based microwave radiometry. *Radio Science*, 1978, vol. 13, no. 4, p. 677-685.
- [15] MARZANO, F. S., CIMINI, D., CIOTTI, P., WARE, R. Modeling and measurement of rainfall by ground-based multispectral microwave radiometry. *IEEE Transactions on Geoscience and Remote Sensing*, 2005, vol. 43, no. 5, p. 1000-1011.
- [16] MARZANO, F. S., et al. Bayesian estimation of precipitating cloud parameters from combined measurements of spaceborne microwave radiometer and radar. *IEEE Transactions on Geoscience and Remote Sensing*, Jan 1999, vol. 37, p. 596-613.
- [17] MARZANO, F. S., et al. Rainfall nowcasting from multi-satellite passive-sensor images using a recurrent neural network. *IEEE Transactions on Geoscience and Remote Sensing*, Nov 2007, vol. 45, p. 3800-3812.
- [18] LIU, G. R., et al. Rainfall intensity estimation by ground-based dual-frequency microwave radiometers. *Journal of Applied Meteorology*, 2001, vol. 40, p. 1035-1041.
- [19] WON, H. Y., KIM, Y., LEE, H. An application of brightness temperature received from a ground-based microwave radiometer to estimation of precipitation occurrences and rainfall intensity. *Asia-Pacific Journal of Atmospheric Sciences*, 2009, vol. 45, no. 1, p. 55 - 69.
- [20] FERRARO, R. R., SMITH, E. A., BERG, W., HUFFMAN, G. J. A screening methodology for passive microwave precipitation retrieval algorithms. *Journal of the Atmospheric Sciences*, 1998, vol. 55, no. 9, p. 1583-1600.
- [21] SKOU, N., LE VINE, D. *Microwave Radiometer Systems: Design & Analysis*. Norwood: Artech House Inc., 1989.
- [22] SHARKOV, E. A. *Passive Microwave Remote Sensing of the Earth, Physical Foundations*. Chichester: Praxis Publishing Ltd, 2003.
- [23] Anemo s.r.o., Czech Republic. *WS981 (manual)*, www.anemo.cz, 56 pages. [Online] Cited 2010-05-15. Available at: <http://www.anemo.cz/dokumenty/WS981navod.zip>.
- [24] SKOFRONICK-JACKSON, G. M., GASIEWSKI, A. J., WANG, J. R. Influence of microphysical cloud parameterizations on microwave brightness temperatures. *IEEE Transactions on Geoscience and Remote Sensing*, Jan 2002, vol. 40, no. 1, p. 187-196.
- [25] WORLD METEOROLOGICAL ORGANIZATION (WMO). *Guide to Meteorological Instruments and Methods of Observation*. Geneva, 2008.
- [26] LONG, D. G., REMUND, Q. P., DAUM, D. L. A cloud-removal algorithm for SSM/I data. *IEEE Transactions on Geoscience and Remote Sensing*, Jan 1999, vol. 37, no. 1, p. 54-62.

About Authors ...

Petr DVORÁK was born in 1985. He received his M.Sc. in Electrical Engineering from the Czech Technical University in Prague in 2009. He is currently working toward the Ph.D. degree in Radio Electronics. His research interests include radiometry, microwave molecular spectroscopy and EMC measurements.

Miloš MAZÁNEK (*1950) received his M.Sc and Ph.D. degrees from the CTU in 1974 and 1980, respectively. He has been a head of the Dept. of Electromagnetic Field (CTU) since 1997. He is a senior member of IEEE, the head of the Radioengineering Society and Czech National URSI Committee. His research interests are in the field of antennas, EMC, microwave radiometry and propagation.

Stanislav ZVÁNOVEC was born in 1977. He received the M.Sc. degree in 2002, Ph.D. degree in 2006 and defended the habilitation thesis in 2010 at the Czech Technical University in Prague. To date, he is an associate professor at the Department of Electromagnetic Field at the CTU in Prague. His current research interests include electromagnetic wave propagation issues for millimeter wave band as well as quasioptical and free space optical systems. He is chair of Joint MTT/AP/ED/EMC chapter of the IEEE Czechoslovakia Section and head of the Commission F of the Czech National URSI Committee.